J. Fluid Mech. (1973), *vol.* 58, *part* 1, *pp.* 97–114
Printed in Great Britain

High Reynolds number flow past an equatorial island

By ROSS HENDRY
Massachusetts Institute of Technology and Woods Hole Oceanographic Institution
AND CARL WUNSCH
Department of Earth and Planetary Sciences, Massachusetts Institute of Technology

(Received 2 November 1972)

A survey of the density field in the immediate vicinity of Jarvis Island was made in April 1971. The island is isolated and is situated in the Pacific Equatorial Undercurrent, thus presenting the opportunity to study a high Reynolds number ($\sim 10^9$) stratified shear flow. Large deflexions of the isopycnals were observed near the island. Solutions derived from the perfect-fluid equations of Drazin (1961) are in reasonable agreement with the observed mass field in the upstream region. Downstream, a wake region was apparent, but the dynamics of the wake are obscure. A coefficient of pressure deficit in the wake is in the same range as values computed from homogeneous laboratory flows, but baroclinic effects are observed.

1. Introduction

We wish to report on a survey that was made of the adjustment of the Pacific Equatorial Undercurrent to the presence of an island obstacle. The work is complementary to a study of the flow about Bermuda, reported by Hogg (1972) and Wunsch (1972). At Bermuda the adjustment process is dominated by Coriolis effects and complicated by time variability in the exterior conditions. Jarvis Island, located at 0° 23′ S, 160° 00′ W in the central equatorial Pacific Ocean, provided an opportunity to study the opposite extreme, in which the earth's rotation appeared negligible and the exterior conditions could be assumed to be steady. The cruise, leg 4 of the Aries expedition of the Scripps Institution of Oceanography, was under extreme time pressure and the survey reported here is incomplete in many ways. None the less, sufficient information was obtained to provide an interesting example of an extremely high Reynolds number flow. Since the ocean is stratified, and the mean flow sheared, the conditions are more complicated than in equivalent laboratory situations, but an attempt to understand the flow is worth while since it appears to be difficult to obtain such high Reynolds numbers in the laboratory. The measurements may also have applicability to the study of the flow past small seamounts at mid-latitudes, or, in the atmosphere, of flow past mountains, if the Rossby number is sufficiently large.

In April 1971 a survey of temperature and salinity was made about Jarvis Island, an isolated island in the central Pacific Ocean. The main feature of the oceanic circulation in this region is the Pacific Equatorial Undercurrent (see,

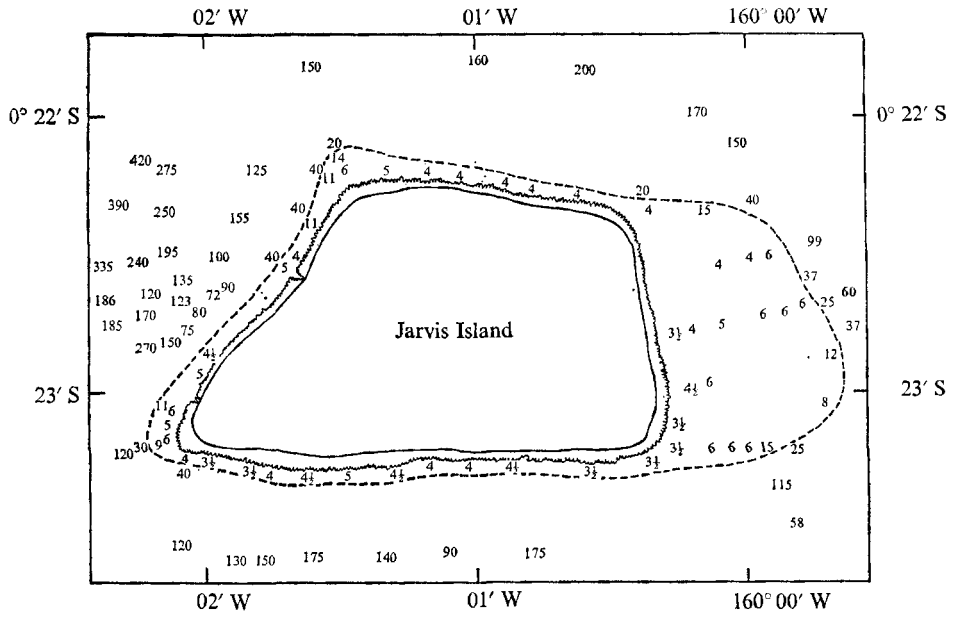

FIGURE 1. Chart of water depths (in fathoms) surrounding Jarvis Island (after C. and G.S. 4193). One minute of latitude or longitude is one nautical mile (1·85 km).

for example, Knauss 1960), an intense eastward subsurface flow confined to the top few hundred metres with a maximum speed of order 100 cm s^{-1}. This highly sheared current has a velocity maximum at a depth near 150 m in this area, and is embedded in the main thermocline where the stratification is greatest. Taft *et al.* (1973) discuss the general features of the equatorial circulation during the expedition.

The presence of Jarvis Island in the equatorial flow produced marked effects on the density field. The Reynolds number of the flow based on the island dimensions is about 10^9 – higher than has been achievable in the laboratory. A distinct wake-like effect was observed in the downstream flow. We shall show that an ideal-fluid model of Drazin (1961) is in fair agreement with the observations outside the wake region.

2. Observations

Measurements at a total of 34 STD (salinity–temperature–depth) stations were taken about Jarvis Island in a 2-day period early in April 1971, from the R.V. *Thomas Washington* as part of the Scripps 'Aries' expedition. A chart of the island and the known water depths is given in figure 1. The island is roughly elliptical in shape with a major axis of length 4 km aligned east–west in the direction of the Undercurrent flow, and a minor axis of length 2 km.

The water column showed several distinctive features which are characteristic of this equatorial region and are partly related to the Undercurrent. An example of measurements from an STD station is shown in figure 2. Typically, the top

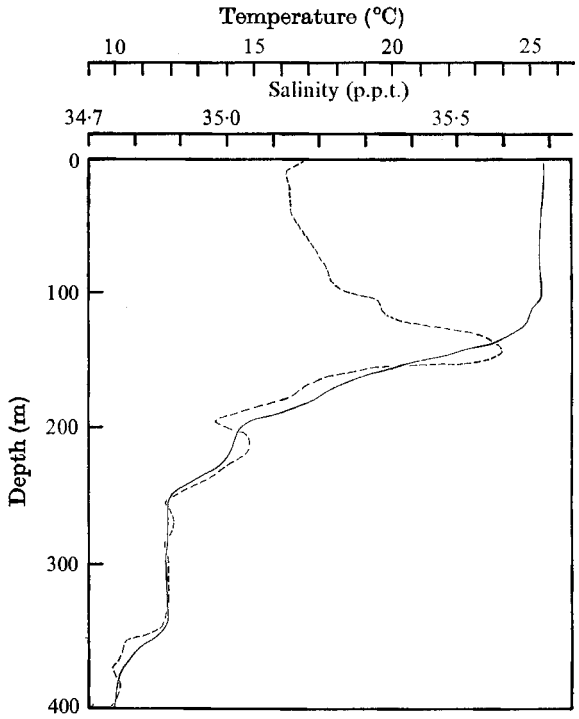

FIGURE 2. 'Typical' temperature (solid line) and salinity (broken line) profiles on the equator far from the island. A surface mixed layer and a strong salinity maximum are the most prominent features.

100 m of water was very homogeneous in temperature at near the surface value of 25·5 °C. A sharp, fairly linear thermocline across which the temperature drops to 15 °C was found between 100 and 200 m. In the deeper water the temperature gradient gradually decreases, and the temperature itself is typically near 5 °C at 1000 m. A salinity maximum associated with the Undercurrent south of the equator was found at a depth near 120 m with values in excess of 35·6 p.p.t. The salinity decreases to about 35·2 p.p.t. at the surface, and in the deeper water near 500 m values of 34·7 p.p.t. were observed. The density of the water is controlled effectively by the temperature alone.

Figure 3 shows the profile of velocity obtained during the expedition at 150° W and described in detail by Taft *et al.* (1973). Owing to the time problem alluded to, a planned profile was not obtained at Jarvis Island itself. We shall use the 150° W profile and the consequences of the longitudinal difference will be discussed further below. Note the strong easterly flow with maximum at 115 m characteristic of the Undercurrent. Under 'normal' conditions, the surface layer (down to about 20 m) in this area is believed to move westward as the South Equatorial Current. The anomalous behaviour shown in figure 3 was confirmed at Jarvis Island by the ships' drift and radar navigation off the island.

Near Jarvis Island a strong signal was imposed on the general temperature and salinity characteristics. First we describe the distortion of the temperature field, and then the characteristics of the 'dynamic depth' field, an integrated

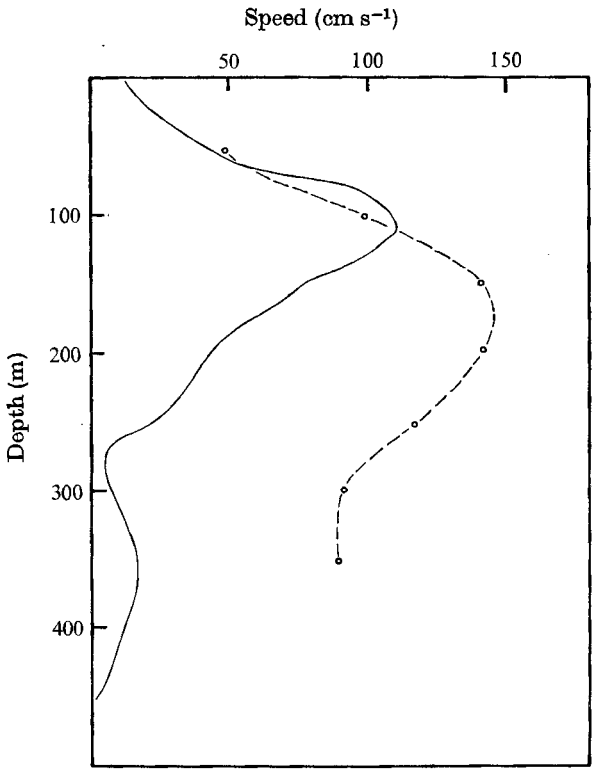

FIGURE 3. Zonal (eastward) component of velocity as a function of depth measured at 150° W on the equator by Taft *et al.* (1973). The dashed line gives an estimate of the flow at 160° W just upstream of Jarvis Island.

quantity (related to the pressure field) with dynamical significance, will be discussed.

From figure 4(*a*) it is clear that station keeping by the ship was remarkably poor during some watches. Since we shall confine our study to the upper 500 m of water and the 'down-traces' of the STD stations, the starting positions of the stations are a reasonable representation of their position. Some spatial smearing is inevitably involved in our results. The survey was intermittently conducted over 2 days with other programmes intermixed. Thus, some degree of time smearing was also introduced. For our purposes, we believe that the flow may be considered steady. Details of variability in the mean flow are discussed by Taft *et al.* (1973). We have no information on variability in the secondary flow.

The isothermal surfaces are displaced from their ambient level around the island, the displacements being of the order of tens of metres and sometimes greater than 100 m (see figures 4*a*, *b*, *c*). The effects are roughly symmetric about the east–west flow axis but not symmetric about the island in the flow direction. Judging from the outermost stations, the effects of the island on the isotherms are confined to within 5 km of the centre of the island in lateral extent and upstream of the island, while downstream they extend 10 km or more in a wake-like manner.

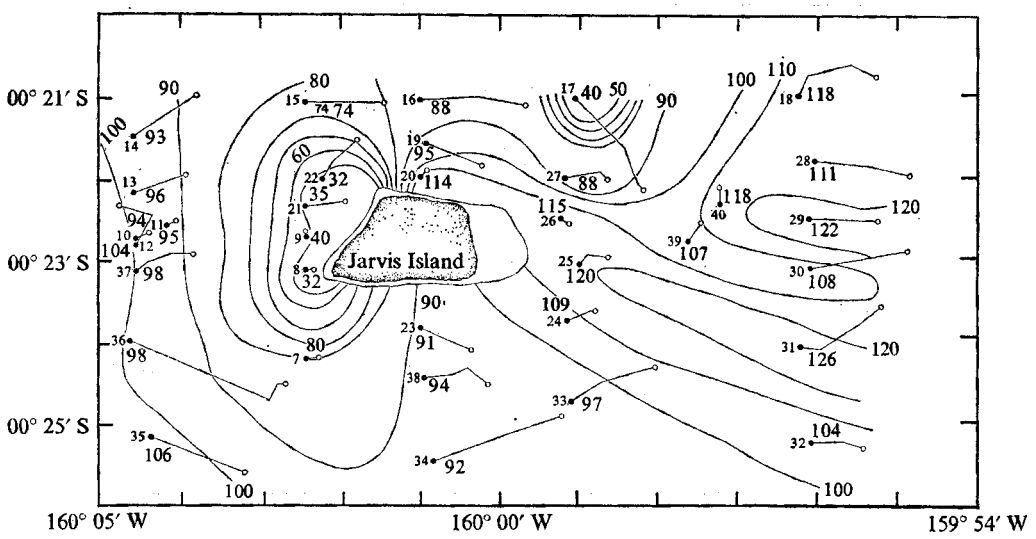

(*a*)

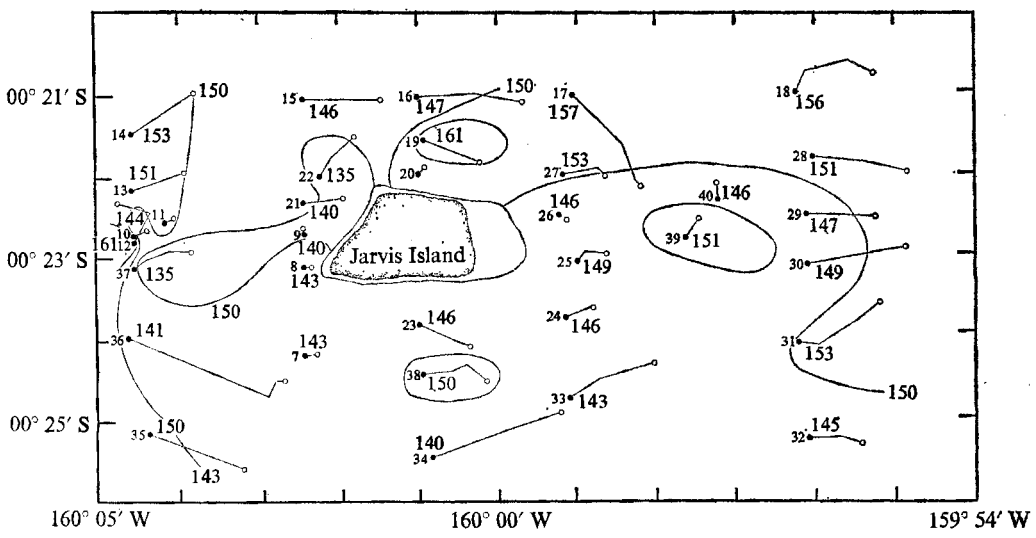

(*b*)

FIGURES 4(*a*), (*b*). For legend see next page.

The effects are weakest on the 19 and 20 °C surfaces, which lie about 150 m below the surface of the ocean (shown in sections in figure 5). Isotherm displacements also tend to be symmetric in the vertical direction about these surfaces, i.e. if the 21 °C surface rises at a certain spot, the 18 °C surface tends to sink there. Above the 20 °C surface, the isothermal surfaces rise as they approach the island from the west or the upstream direction, with displacements largest on the major axis of the island. The maximum height of a surface above its ambient level occurs just upstream of the island, and the temperature surface then sinks

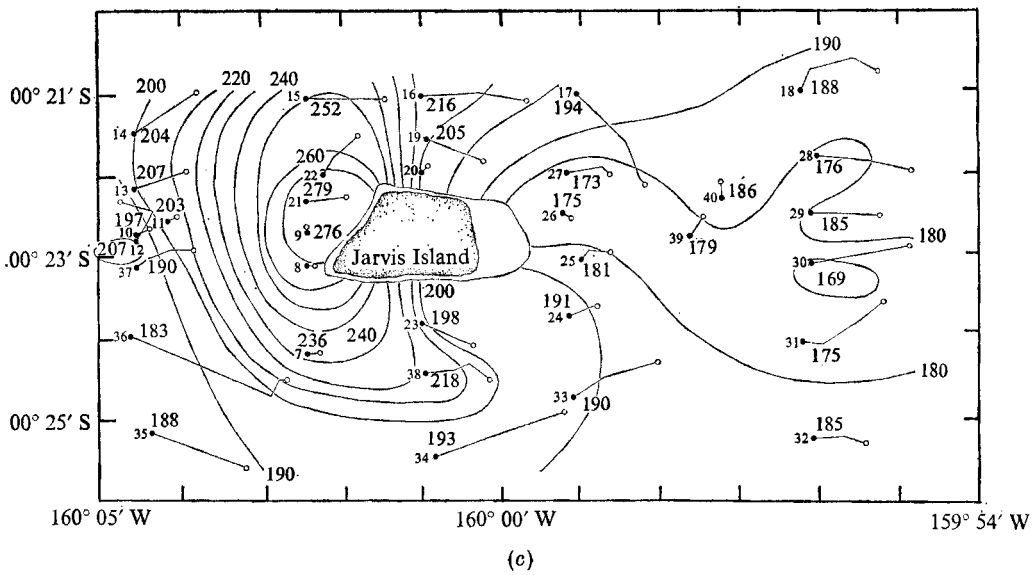

FIGURE 4. Depth in metres of the (*a*) 25° C, (*b*) 20 °C and (*c*) 15 °C isotherms at Jarvis Island. The station positions on this and subsequent figures are shown as smaller numbers. The station starting position is given by the solid dot, end position by the open dot, and the track between is also indicated. The contour interval is 10 m.

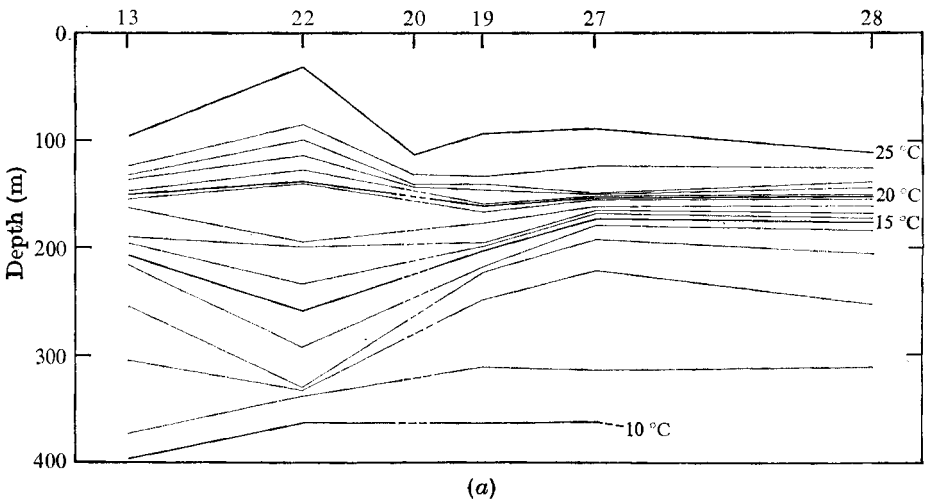

FIGURE 5. (*a*) For legend see facing page.

rapidly along the island perimeter. Below the 20 °C surface this pattern is reversed, with the result that, as the island is approached from upstream, the isotherms diverge in the vertical direction and the thermocline becomes more diffuse. Around the upstream shoulders of the island, the thermocline recontracts sharply, with the isotherm surfaces regaining their ambient level with some overshoot. Outside the region directly behind the island, the isotherm surfaces very gradually flatten out to their far-upstream form.

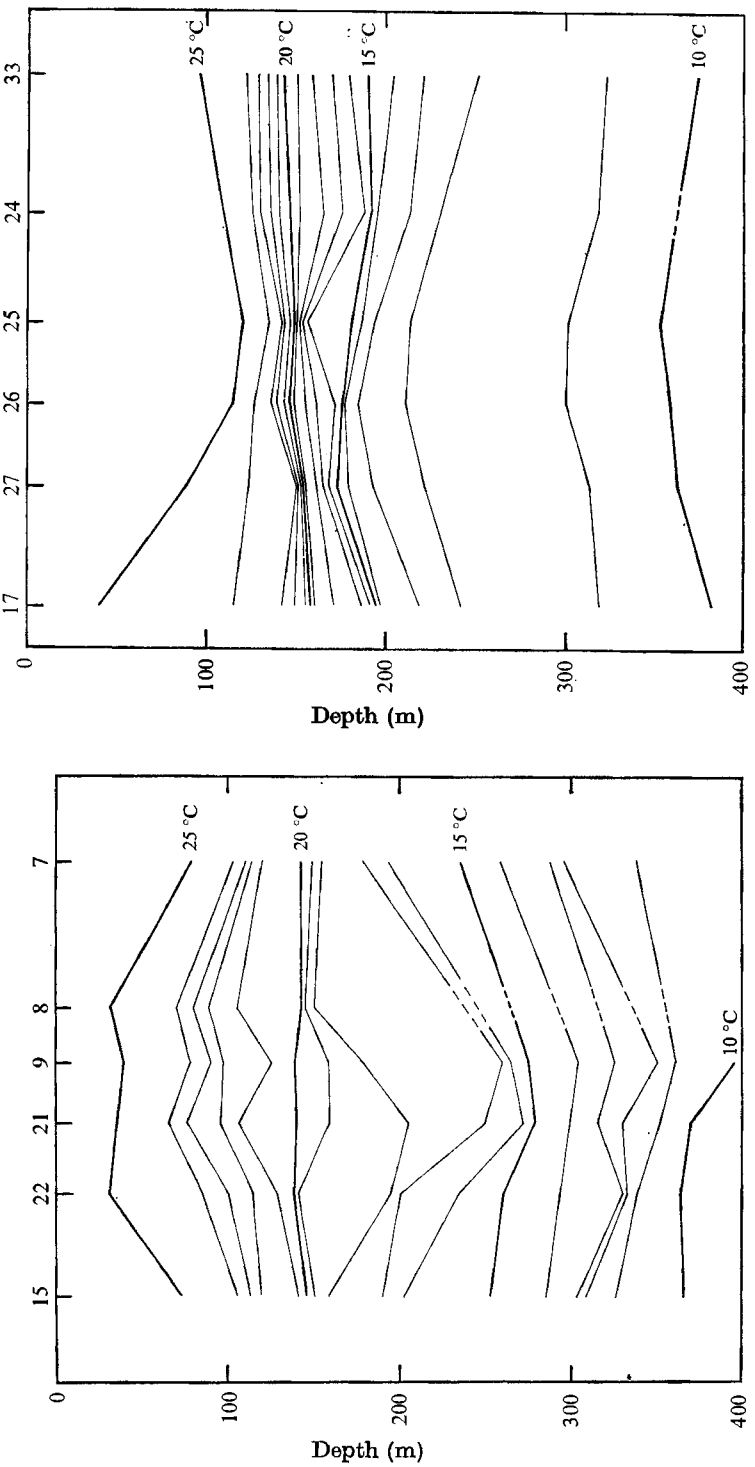

FIGURE 5. (*a*) East–west section of temperature made along the northern edge of the island. Station positions are indicated at the top. (*b*) North–south section of temperature taken along the western side of Jarvis Island. The thermocline is seen to be very diffuse. (*c*) North–south section of temperature taken along the eastern side of the island. The thermocline is now very sharply defined.

Directly downstream of the island, however, the thermocline is observed to contract even more, giving a very strong gradient near 150 m and a somewhat weaker gradient higher or lower than this level, which is centred near the 20 °C surface. This sharp thermocline diffuses somewhat with increasing distance downstream from the island. The horizontal temperature gradients are much reduced in the wake.

Unfortunately no direct velocity measurements are available in the area of Jarvis Island, and historical data for the region 160° W on the equator is very sparse. The measurements taken at 150° W in April 1971 (figure 3, see also Taft *et al.* 1973) show the level of zero vertical shear, or maximum east–west speed in the Undercurrent, to be at a depth of 116 m. It is known that the Undercurrent core rises towards the east, the level of maximum speed being associated with water of a well-defined density (300 cl/t specific volume anomaly; see Tsuchiya 1968). In fact, at 150° W, the 300 cl/t surface was found at exactly 116 m, where the temperature was 21·89 °C and the salinity 35·90 p.p.t. At station 35 upstream of Jarvis Island, where the temperature and salinity are believed to be relatively unaffected by the island, this 300 cl/t surface was observed to lie at 148 m (corresponding to 20·37 °C and 35·36 p.p.t.). We shall accept this as an estimate of the level of zero shear in the undisturbed flow near the island, a critical point in the theory. An estimate of the profile upstream of Jarvis Island is shown in figure 3 as a dashed line.

Another problem in the interpretation of the observations is the speed of the surface flow and the associated deformation of the free surface. It is believed that this effect is relatively small compared with the baroclinic effects, which is true for a surface speed less than about 26 cm s^{-1}. However, this is a difficult and unfortunately unresolved point.

Instead of examining the dynamics of the flow in terms of pressure gradients on a given horizontal surface, the 'dynamic depth' of a given constant-pressure surface relative to the sea surface or atmospheric pressure will be used for convenience, as is common in physical oceanography. The dynamic depth D is defined as

$$D = \int_{P_{\text{atm}}}^{p} \alpha(x, y, p')\, dp' \tag{1}$$

in units of 'dynamic metres', where α is the specific volume of the water in cm^2/g, p the pressure level in decibars and x and y are horizontal co-ordinates. P_{atm} is the atmospheric pressure at the sea surface. The hydrostatic approximation is assumed, so that

$$\frac{\partial p}{\partial z} = -\frac{1}{\alpha}\frac{\partial \phi}{\partial z}, \tag{2}$$

where $\phi(z)$ is the geopotential of the earth. Then the equations of inviscid steady fluid motion can be written in (x, y, p) co-ordinates as

$$\mathbf{u}.\nabla\mathbf{u} = -g\nabla_H \zeta + \nabla_H D, \tag{3}$$

where ζ is the sea surface elevation (depending upon the particular units used, a numerical scale factor may have to be introduced into the equation; see Sverdrup, Johnson & Fleming 1942).

If on some pressure surface the velocity vanishes or is everywhere constant, the elevation of the free surface can be obtained from the dynamic depth field at that level. However, no such level is obvious in the Jarvis Island data. Since the dynamic depth is an integrated quantity, the computed values will be very stable, and resolution of better than 1 dynamic centimetre is easily obtained. If the free surface is flat or has negligible slope compared with the effects of internal processes, the dynamic depth field is analogous to the pressure field in a homogeneous flow, with high pressure corresponding to low dynamic depth and vice versa.

Equation (3) can be rewritten as

$$(\nabla \times \mathbf{u}) \times \mathbf{u} = -\nabla\{-\tfrac{1}{2}\mathbf{u}.\mathbf{u} + g\zeta - D\}, \tag{4}$$

and the Bernoulli quantity B, defined by

$$\tfrac{1}{2}\mathbf{u}.\mathbf{u} + g\zeta - D \equiv B, \tag{5}$$

is conserved along streamlines.

If there is no obvious 'level of no motion' the interpretation of such a flow becomes confused since the pressure field is quadratic in the velocity and a simple decomposition into barotropic and baroclinic components is not possible.

To obtain the free-surface effect from the overall velocity field is difficult, but it can be estimated using the results for homogeneous potential flow with a free surface. At the forward stagnation point of such a flow about an obstacle

$$g\zeta = \tfrac{1}{2}U^2,$$

where U is the speed far upstream. For a 20 cm s^{-1} surface current this gives a 0·2 cm rise, while a 50 cm s^{-1} flow leads to a 1·25 cm rise. The value for the Jarvis Island case probably lies somewhere between. If it is close to the lower value (as we shall assume) the free-surface effect is negligible in comparison with the noted baroclinic effects, but the neglect of the surface flow is a possible difficulty with the treatment given below.

Dynamic depth field

Instead of considering D itself, the departure of D from a standard value is used. In fact, if $\alpha(T, S, p)$ is the specific volume of the water at its actual temperature, salinity and pressure, then the specific volume anomaly

$$\delta(T, S, p) = \alpha(T, S, p) - \alpha(0\,^{\circ}\mathrm{C}, 35\,‰, p)$$

is integrated to give the dynamic depth anomaly ΔD. Since only horizontal gradients of D are significant, the two quantities are dynamically identical. At the free surface ΔD is defined to vanish. At a given pressure a high value of ΔD at one horizontal location indicates generally less dense water in the column above that level, relative to a neighbouring horizontal position on that level. Since 1 m of seawater adds nearly 1 decibar to the pressure, the decibar is a convenient unit for pressure.

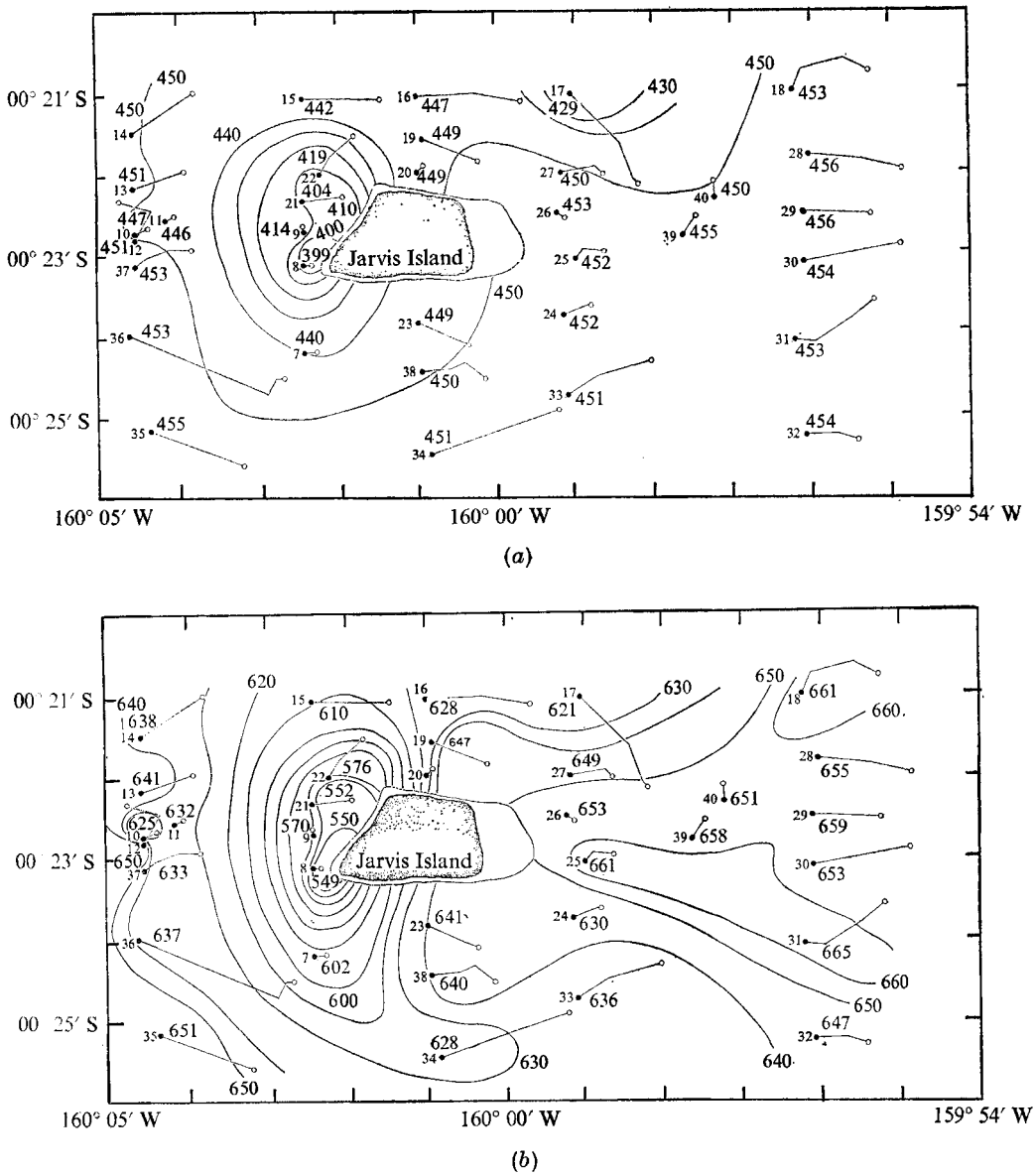

FIGURES 6(*a*), (*b*). For legend see facing page.

The observations about Jarvis Island are presented in figure 6(*a*)–(*d*) at levels from 100 to 350 decibars. At 100 decibars the region of low D at the upstream end of the island represents the effect of cooler water rising into the top 100 m or so in this area. This effect is confined to the immediate upstream end and the flat dynamic topography downstream of the island is notable. The total relief is 5·4 dynamic cm – a large baroclinic signal (1 dynamic cm = 10^{-2} dynamic metres). At 150 decibars there is a very pronounced region of low D (high pressure) at the immediate upstream end of the island. The distortion of the con-

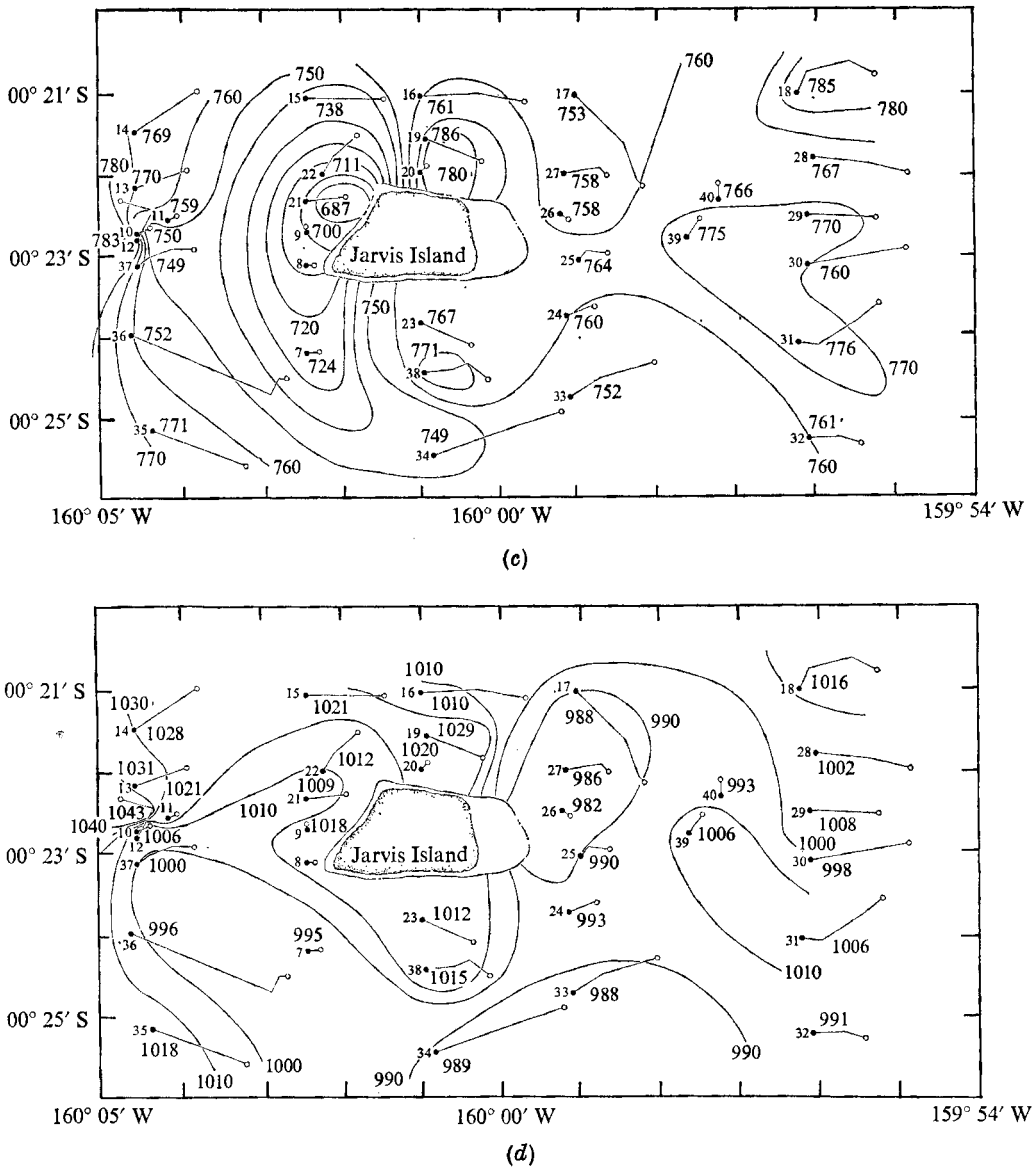

FIGURE 6. Dynamic depth of (*a*) 100, (*b*) 150, (*c*) 200 and (*d*) 350 decibar surfaces relative to the sea surface. Units are dynamic millimetres (10^{-3} dynamic metres), and the contour interval is 10 dynamic millimetres.

tours downstream of the island and the relatively flat dynamic topography there illustrate the wake-like effect. At 150 decibars the dynamic topography thus represents the full integrated effect of the upper region. There is a relief of 11·6 dynamic centimetres at this level, the highest gradients in dynamic depth observed.

Between depths of 150 and 200 m, relatively warm water from far upstream sinks as it moves towards the upstream end of the island. This warm water tends

to reduce the region of low dynamic depth at the 200 decibar level (figure 6*c*) just upstream. Noticeable for the first time at the 200 decibar level are areas of relatively great dynamic depth near the sides of the island. There is a suggestion of a region where D is slightly higher just downstream of the island, and again the wake-like upstream–downstream asymmetry is apparent. The dynamic relief on the 200 decibar surface is 9·9 dyn cm, and the relatively small reduction in this figure from that for the 150 decibar surface ($-1{\cdot}7$ dyn cm) compared with the large increase from 100 to 150 decibars ($+6{\cdot}2$ dyn cm) illustrates the greater activity occurring in the top layer, i.e. the greater shear in the velocity profile there. The picture obtained at 200 decibars (figure 6*c*) is qualitatively unchanged upstream, but a distinct region of low dynamic depth is formed downstream. At 350 decibars the coherent pattern noted in the higher level begins to disintegrate (figure 6*d*), and by 500 decibars (not shown) becomes quite confused. There is a residual region of low D at the upstream end of the island but not much more can be said. At the 150 and 200 decibar levels the region where D is slightly higher downstream of the island is related to the contraction of the thermocline directly downstream of the island, which will be discussed below.

3. Interpretation

The flow around Jarvis Island is characterized by a very high Reynolds number:

$$R = UL/\nu \sim 10^9,$$

where $U = 100\ \mathrm{cm\ s^{-1}}$ and $L = 10^5$ cm are a velocity and length scale respectively, and $\nu = 10^{-2}\ \mathrm{cm^2-s^{-1}}$ the kinematic viscosity of water. Experiments on laboratory flows around obstacles have approached $R = 10^7$ for homogeneous fluids (Roshko 1961) and even at these high Reynolds numbers the upstream mean flow closely resembles potential flow. Downstream there are pronounced wake effects due to separation of the flow from the sides of the obstacle. The Jarvis Island flow is, however, also highly stratified and vertically sheared. The experiments of Hawthorne & Martin (1955) may have some relevance to the case at hand, but the full complexity of the Jarvis Island flow will not be easily duplicated in the laboratory.

During this same expedition, measurements of the small-scale turbulence of the free undercurrent (at 100 m, 1° N, 158° W) were made by Gibson & Williams (1972). They detected an inertial subrange with dissipation rate $\epsilon = 0{\cdot}04$–$0{\cdot}16\ \mathrm{cm^2\ s^{-3}}$, which should be a good estimate of the intensity of the irregularities of the current incident on Jarvis Island.

Wunsch (1972) reported that at Bermuda the temperature and velocity 'microstructure' increased as the island is approached. He related this microstructure to dissipation of the mean flow at the island. A similar, but more complicated, microstructure gradient exists at Jarvis Island, and to the extent that this structure represents viscosity and diffusion, the perfect-fluid model used here will be incorrect.

Since the island latitude is 0° 23′ S, the Rossby number is

$$R_0 = U/fL \sim 10^2/10^{-6} \times 10^5 = 10^3,$$

where $f = 2\Omega \sin$ (latitude) and Ω is the rotational frequency of the earth. Thus to a good first approximation rotational effects will be unimportant in the dynamics of the Jarvis Island flow.

Consider then an ocean unbounded in horizontal extent, with a free surface, and an obstacle, which is taken to have vertical sides, situated at the origin. Jarvis Island is very steep, though a general survey is lacking (see figure 1). Far from the obstacle the current $U(z)$, flowing in the positive-x direction, and the density $\rho(z)$ are specified. We assume no diffusive or viscous effects, and the flow is incompressible.

The appropriate boundary conditions are

$$\mathbf{u}(x,y,z) \to U(z)\nabla x, \quad \rho(x,y,z) \to \rho_0(z) \quad \text{as} \quad x^2+y^2 \to \infty, \tag{6}$$

$$\mathbf{u}.\mathbf{n} = 0 \quad \text{on the surface,}$$

n being the normal, and $p = 0$ at $z = \zeta(x,y)$, where atmospheric pressure fluctuations are neglected.

Following Drazin (1961), the momentum equations can be written as

$$\boldsymbol{\omega} \times \mathbf{u} = -\nabla H - p\rho^{-2}\nabla\rho, \tag{7}$$

where $\boldsymbol{\omega} = \nabla \times \mathbf{u}$ is the vorticity and

$$H = p/\rho + gz + \tfrac{1}{2}\mathbf{u}.\mathbf{u} \tag{8}$$

is the Bernoulli 'head'.

Then $\mathbf{u}.\nabla H = 0$ and the head is conserved along a streamline and is a function of the upstream level of the streamline alone. The equations may be reformulated in terms of z_0, the height of a streamline far upstream, instead of the pressure. Specifying z_0 specifies a particular density also, and

$$\nabla\rho = (d\rho/dz_0)\nabla z_0,$$

where $d\rho/dz_0$ is to be evaluated far upstream.

By non-dimensionalizing the equations by the velocity scale V and a height scale h, Drazin arrives at the expression

$$\boldsymbol{\omega} \times \mathbf{u} = -\{J(z-z_0) - \tfrac{1}{2}L(U^2 - \mathbf{u}.\mathbf{u}) + M\}\nabla z_0, \tag{9}$$

where

$$J = N^2/(V/h)^2, \quad L = -\frac{h}{\rho}\frac{d\rho}{dz_0}, \quad M = U\frac{dU}{dz_0}\Big/(V^2/h)$$

and $N^2 = (-g/\rho)\,d\rho/dz_0$ is the square of the buoyancy (Brunt–Väisälä) frequency. The vorticity balance

$$\mathbf{u}.\nabla\boldsymbol{\omega} = \boldsymbol{\omega}.\nabla\mathbf{u} - J\nabla z \times \nabla z_0 - \tfrac{1}{2}L\nabla(\mathbf{u}.\mathbf{u}) \times \nabla z_0 \tag{10}$$

gives the changes of vorticity along a streamline due to the stretching of vorticity and gravitational and dynamic torques working on the stratification. L is of order 10^{-3} and the term multiplied by L will be neglected. Near Jarvis Island N was found to be near $10^{-2}\ \mathrm{s}^{-1}$ in the main thermocline between depths of 50 and 250 m. The vertical shear dU/dz is estimated to be near $10^{-2}\,\mathrm{s}^{-1}$ as well. An appropriate vertical scale height for both the stratification and shear is 100 m.

Thus the dimensionless parameters J and M both become of order unity, making a perturbation scheme difficult to apply. Lighthill (1956) treated the case $J \ll M \ll 1$, while Drazin (1961) dealt with thecomplementary limit $J \gg 1$, where stratification is dominant. The flow around Jarvis Island may exhibit characteristics brought out in both these studies, since the upper 50 m is nearly homogeneous and strongly sheared, while in the thermocline the stratification is large. Since the Jarvis Island survey gave only the temperature and salinity fields, the velocity field must be inferred by its effects on the measured quantities. Because of the nature of the measurements no signal will be received from the homogeneous surface layer even though the vertical component of velocity may be large there. The level of zero shear in the Equatorial Undercurrent, where the eastward component of velocity is a maximum, lies in the main thermocline, near depths of 150 m at Jarvis Island. At this level the parameter M vanishes, while the parameter J reaches a maximum of perhaps 4. This central region gives a strong density signal and the high Richardson number limit of Drazin (1961) seems applicable, even if only in some limited vertical region about the zero shear level. We shall therefore study this limiting case. It is found that, despite the use of the theory outside its obvious range of validity, the agreement with the observations is quite good.

In (9) the various quantities are expanded in an asymptotic series in powers of the inverse Richardson number J^{-1} as

$$\mathbf{u} = \mathbf{u}_1 + J^{-1}\mathbf{u}_2 + \ldots,$$
$$\boldsymbol{\omega} = \nabla \times \mathbf{u} = \boldsymbol{\omega}_1 + J^{-1}\boldsymbol{\omega}_2 + \ldots,$$
$$z_0 = z_1 + J^{-1}z_2 + \ldots.$$

Like powers of J^{-1} are collected, giving a series of closed problems.

The presence of the supposed large number J itself in (9) yields an immediate constraint:

$$0 = -(z - z_1)\nabla z_1.$$

Since $z_0 \to z$ as $x^2 + y^2 \to \infty$, this gives $z_1 = z$. The assumption of overpowering stratification forces the first approximation to the flow to be exactly horizontal, consisting of two-dimensional flows about the obstacle in horizontal planes.

The solution can be written as

$$\mathbf{u}_1 = U(z_0)\nabla\phi_1(x, y),$$

where
$$\frac{\partial^2\phi_1}{\partial x^2} + \frac{\partial^2\phi_1}{\partial y^2} = 0 \quad (\phi_1 \to x \quad \text{as} \quad x^2 + y^2 \to \infty) \tag{11}$$

and $\partial\phi_1/\partial\mathbf{n} = 0$ on the surface of the obstacle. Also $\boldsymbol{\omega}_1 = (dU/dz_0)\nabla z \times \nabla\phi_1$. The problem to next order is

$$\begin{aligned}\boldsymbol{\omega}_1 \times \mathbf{u}_1 &= (z_2 - M)\nabla z \\ &= (dU/dz_0)\, U(\nabla z \times \nabla\phi_1) \times \phi_1 \\ &= -Mq_1^2\nabla z,\end{aligned}$$

where $q_1 = |\nabla\phi_1|$. Then immediately

$$z_2 = M(1 - q_1^2) \tag{12}$$

and
$$z - z_0 = J^{-1}M(q_1^2 - 1) + O(J^{-2}). \tag{13}$$

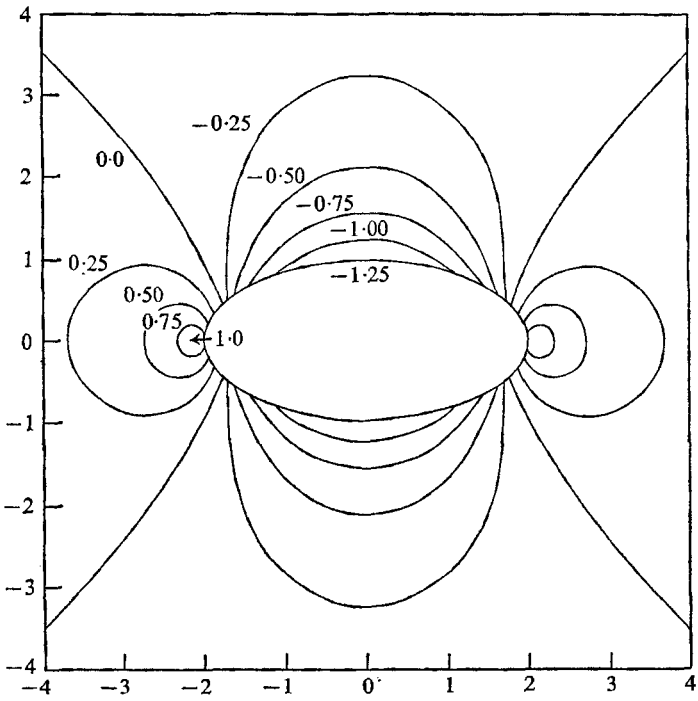

FIGURE 7. Contours of $1-q_1^2$ as computed from the potential flow solution of Lamb (1932). Reversal in sign corresponds to a reversal in sign of the isotherm displacements. Units are non-dimensional.

When $M < 0$, i.e. when the velocity U is positive and the shear negative in particular, corresponding to the water above 150 decibars, it is seen that a density surface (streamline surface) rises above its ambient level when $q_1^2 < 1$, or where the horizontal potential flow has less kinetic energy than the upstream flow. This deceleration occurs near the upstream and downstream ends of the obstacle, at about the points where the flow should stagnate. When the flow speeds up at the sides of the obstacle the density surface sinks below its ambient value. When the sign of the shear is changed, the direction of flow remaining the same, the density surface displacement has the opposite sign. This result is a Bernoulli effect for sheared stratified flows and depends on the direct interaction between these two quantities. The scale of the displacement of a density surface is

$$J^{-1}M = U\frac{dU}{dz_0}\Big/N^2h$$

in dimensionless units, and just $UN^{-2}(dU/dz_0)$ in dimensional units.

This scale is of order 10^4 cm for the Jarvis Island values, which is quite comparable with the observed isotherm displacements. Equation (13) permits a direct comparison between the observed and computed isopycnal displacement. In figure 7 contours of relative kinetic energy $1-q_1^2$ are drawn, for the case of an elliptical obstacle with eccentricity $\frac{1}{2}$. These contours were obtained by solving

(11) (Lamb 1932). Comparison between figure 7 and, say, figure 4 (*a*) shows surprisingly good agreement between theory and experiment in structure as well as magnitude (outside the wake region).

In terms of dynamic height, on a streamline, we have from (4)

$$\tfrac{1}{2}\mathbf{u}.\mathbf{u}+g\zeta-D=\tfrac{1}{2}U^2-D_0,$$

where U and D_0 are values far upstream, and the difference between a streamline surface and a constant-pressure surface is of second order in this quasi-horizontal flow. In the model then,

$$D-D_0=g\zeta+\tfrac{1}{2}U^2(q_1^2-1). \tag{14}$$

The expected differences in dynamic height on a pressure surface have the scale $U^2/2000$ dynamic centimetres, which for $U = 100\,\mathrm{cm}^{-1}$ gives a reasonable value of 5 dynamic centimetres.

At the upstream end the rapid changes in the theoretical solution duplicate the observations. As the flow accelerates around the sides of the obstacle, there is a reversal in sign of $1-q_1^2$ and another extremal at the midpoints, as seen in the deeper levels around the island. Comparison of figure 7 with figure 6 (*b*) shows the close resemblance between theory and observation.

A new, but somewhat artificial, problem could be posed by imagining some likely form of the wake and then solving the potential flow problem in the exterior region, with no flow into or out of the wake region. Clearly, this could qualitatively reproduce the observed field.

4. The wake

The wake region is perhaps the most interesting and certainly the most complicated. The most striking feature in the wake immediately downstream of the island is the sharp contraction of the thermocline there (e.g. figure 5) and its subsequent broadening in both the downstream and cross-stream direction. Experiments on wakes in stratified fluids (e.g. by Schooley & Stewart 1963; Stockhausen, Clark & Kennedy 1966) have revealed the interesting phenomenon of 'wake collapse'. Directly behind the obstacle, mechanical mixing interchanges fluid particles in both the horizontal and vertical directions, and some of the turbulent kinetic energy is converted to potential energy as heavy particles are raised. This mixing occurs on a macroscopic scale and individual globules of water retain their identity as they are carried further downstream in the wake. The intensity of turbulence decreases away from the obstacle and at some point the mixing energy drops below the level needed to support these heavier particles in their unstable configuration. Gravitational forces act on the heavy particles and wake collapse occurs.

The thinning of the thermocline at stations 25, 26 and 27 about 1 km downstream of Jarvis Island may be an indication of wake collapse. The uncertainty of extrapolating from laboratory geometries and parameter ranges to the oceanic case should be obvious.

We have no information on the wake far downstream, but should like to make the following comments. There have been a number of recent reports of supposed

Pressure level (decibars)	50	100	150	200	250	300
C_p	0·6	0·04	0·01	−0·3	−0·6	−0·8

TABLE 1. Pressure deficit coefficient C_p, as defined in text, as a function of depth in decibars.

von Kármán vortex streets behind islands in the atmosphere (e.g. Chopra & Hubert 1965) and in the ocean (Barkley 1972). However, as can be seen from the figures displayed here, the process of flow adjustment around Jarvis Island (as also for Bermuda) is distinctly three-dimensional. It is very difficult to see how the specifically two-dimensional vortex street can be related to the three-dimensional generation characteristic of islands. A similar view has been expressed by Berger & Wille (1972), who point out that apparent surface manifestations of vortex streets may be very misleading. Attaching the precise terminology 'vortex street' to what is in all probability a very different phenomenon only serves to obscure the subject. A proper observational programme of far-field geophysical wakes remains to be done.

Pressure deficit

One quantity often measured in laboratory experiments on high Reynolds number flows around obstacles is the pressure deficit in the wake, defined as

$$C_p = (P_\infty - P_1)/\tfrac{1}{2}\rho U^2,$$

where P_1 is the pressure at the rear stagnation point and P_∞ and U the pressure and stream speed far upstream respectively. In homogeneous flows around cylinders the pressure at the sides of the obstacle drops as the flow accelerates, and viscous effects in the obstacle boundary layer prevent the rear stagnation point pressure from rising a great deal above this level. The pressure deficit decreases sharply at some critical Reynolds number when the flow becomes turbulent and is then a more slowly varying function of Reynolds number for a given obstacle (Roshko 1961). Analogous values of dynamic depth surplus can be calculated at various levels in the Jarvis Island flow (see table 1). The ambient dynamic depth is estimated by averaging values at upstream stations 12 and 13, and the wake value obtained by averaging values from stations 25, 26 and 27. The total head $\frac{1}{2}\rho U^2$ is estimated from the dynamic depth differences between the averages of values from stations 9, 21 and, when available, 8, and the supposed ambient value.

At the highest Reynolds number he reported, 9×10^6, Rosko (1961) obtained a pressure deficit coefficient $C_p = 0{\cdot}7$ for a circular cylinder. The value is higher than would be obtained for a more streamlined obstacle such as an ellipse. At the 50 decibar level, the value of C_p obtained from the Jarvis Island flow in the nearly homogeneous though sheared surface layer is comparable with Roshko's value. In the deeper layers the baroclinic effects make themselves felt and the negative values in the deeper layers correspond to a higher pressure in the wake than far upstream.

We are indebted to Dr Bruce Taft, chief scientist on Aries IV, for his co-operation in making it possible to carry out these measurements. An obvious debt is owed to the captain and crew, and scientific party of the R.V. *Thomas Washington* of Scripps Institution of Oceanography. Barbara Hickey edited all of the data prior to our analysis. The work was supported by the Office of Naval Research under Contract N00014-67-A-0204-0048.

REFERENCES

BARKLEY, R. A. 1972 Johnston Atoll's wake. *J. Mar. Res.* **30**, 201–215.

BERGER, E. & WILLE, R. 1972 Periodic flow phenomena. *Ann. Rev. Fluid Mech.* **4**, 313–340.

CHOPRA, K. P. & HUBERT, L. F. 1965 Mesoscale eddies in wakes of islands. *J. Atmos. Sci.* **22**, 652–657.

DRAZIN, P. G. 1961 On the steady flow of a fluid of variable density past an obstacle. *Tellus*, **13**, 239–251.

GIBSON, C. H. & WILLIAMS, R. B. 1972 Measurements of turbulence and turbulence mixing in the Pacific Equatorial Undercurrent. Presented at *Int. Symp. on Oceanography of the South Pacific*, Wellington, New Zealand (unpublished manuscript).

HAWTHORNE, W. R. & MARTIN, M. E. 1955 The creation of secondary vorticity in the flow over a hemisphere due to density gradient and shear. *Proc. Roy. Soc.* A **232**, 184–195.

HOGG, N. G. 1972 Steady flow past an island with application to Bermuda. *Geophys. Fluid Dyn.* **4**, 55–81.

KNAUSS, J. A. 1960 Measurements of the Cromwell Current. *Deep Sea Res.* **6**, 265–285.

LAMB, H. 1932 *Hydrodynamics*, 6th edn. Dover.

LIGHTHILL, M. J. 1956 Drift. *J. Fluid Mech.* **1**, 31–53.

ROSHKO, A. 1961 Experiments on the flow past a cylinder at very high Reynolds number. *J. Fluid Mech.* **10**, 345–356.

SCHOOLEY, A. H. & STEWART, R. W. 1963 Experiments with a self-propelled body submerged in a fluid with a vertical density gradient. *J. Fluid Mech.* **15**, 83–96.

STOCKHAUSEN, P. J., CLARK, C. B. & KENNEDY, J. F. 1966 Three-dimensional momentumless wakes in density-stratified liquids. *Hydrodynamics Laboratory, M.I.T. Rep.* no. 93.

SVERDRUP, H. U., JOHNSON, M. W. & FLEMING, R. H. 1942 *The Oceans, Their Physics, Chemistry and General Biology*. Prentice-Hall.

TAFT, B. A., HICKEY, B., WUNSCH, C. & BAKER, D. J. 1973 Equatorial currents at 150° W in April 1971. In preparation.

TSUCHIYA, M. 1968 *Upper Waters of the Intertropical Pacific*. Johns Hopkins Press.

WUNSCH, C. 1972 Temperature microstructure on the Bermuda slope with application to the mean flow. *Tellus*, **24** (4), 350–367.